Parvalbumin-Expressing Interneurons Linearly Transform Cortical Responses to Visual Stimuli

Bassam V. Atallah, William Bruns, Matteo Carandini, and Massimo Scanziani

SUPPLEMENTAL EXPERIMENTAL PROCEDURES

Data Analysis

The suppression/activation of PV cells was quantified in two ways: (i) as the change in spontaneous and visually evoked firing rate (average across all orientations at maximal contrast; Figure S2); (ii) In a subset of PV cells Arch mediated suppression and Chr2 mediated activation was quantified as a function of contrast (eight contrast levels for each cell; Figure 2D,E). An identical method was used to quantify how suppression/activation of PV cells impacted Pyr cell spiking responses (Figure S2,2E,F). Additionally, since Pyr cells exhibit orientation selectivity, suppression/activation was quantified as the percentage change in firing rate at the preferred orientation (Figure 3C).

Changes in the tuning properties (OSI, DSI and HWHH) of individual Pyr cells were quantified by bootstrapping. A property was considered to have changes significantly when its value under control conditions differed ($p < 0.05$) from the bootstrapped distribution of the property during photo-stimulation. Bootstrapped distributions were created by computing the sum-of-Gaussians fit for each of 300 resamples. Each resample was performed in a standard manner and consisted of a random set of trials equal in number to the total number of trials recorded. A trial was allowed to be repeated within an individual resample.
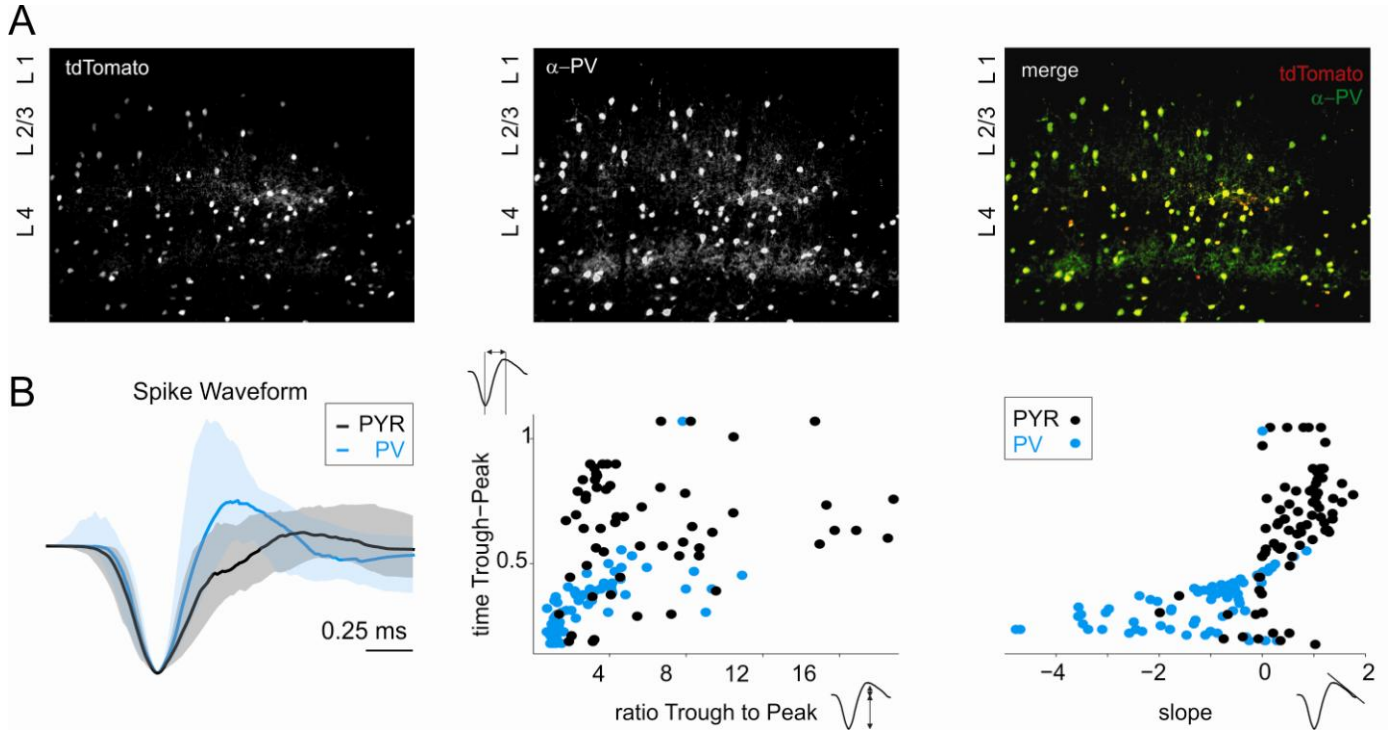
Figure S1: Validation of PV–Cre mouse line (related to Figure 1)

(A) Coronal section of V1 from a PV-Cre x tdTomato mouse. Left, expression of tdTomato; Middle, anti-PV immunstaining. Right, overlay of tdTomato (red) and anti-PV (green). Note that tdTomato expression is detected only in PV expressing cells (97 ± 2%; n = 400 cells in 4 mice).

(B) Left, Average spike waveforms of PV cells (blue; n = 76) and Pyr cells (black; n = 76), shaded area represents the standard deviation. Right, Scatter plot of spike waveform properties (as in Niell & Stryker 2008): the time from trough to peak (y-axis) is plotted against the ratio of the depth of the trough to the height of the peak (middle x-axis) and the slope of the peak 0.6 ms after the trough (right x-axis). Note that PV cells have systematically shorter and faster spikes as compared to Pyr cells.
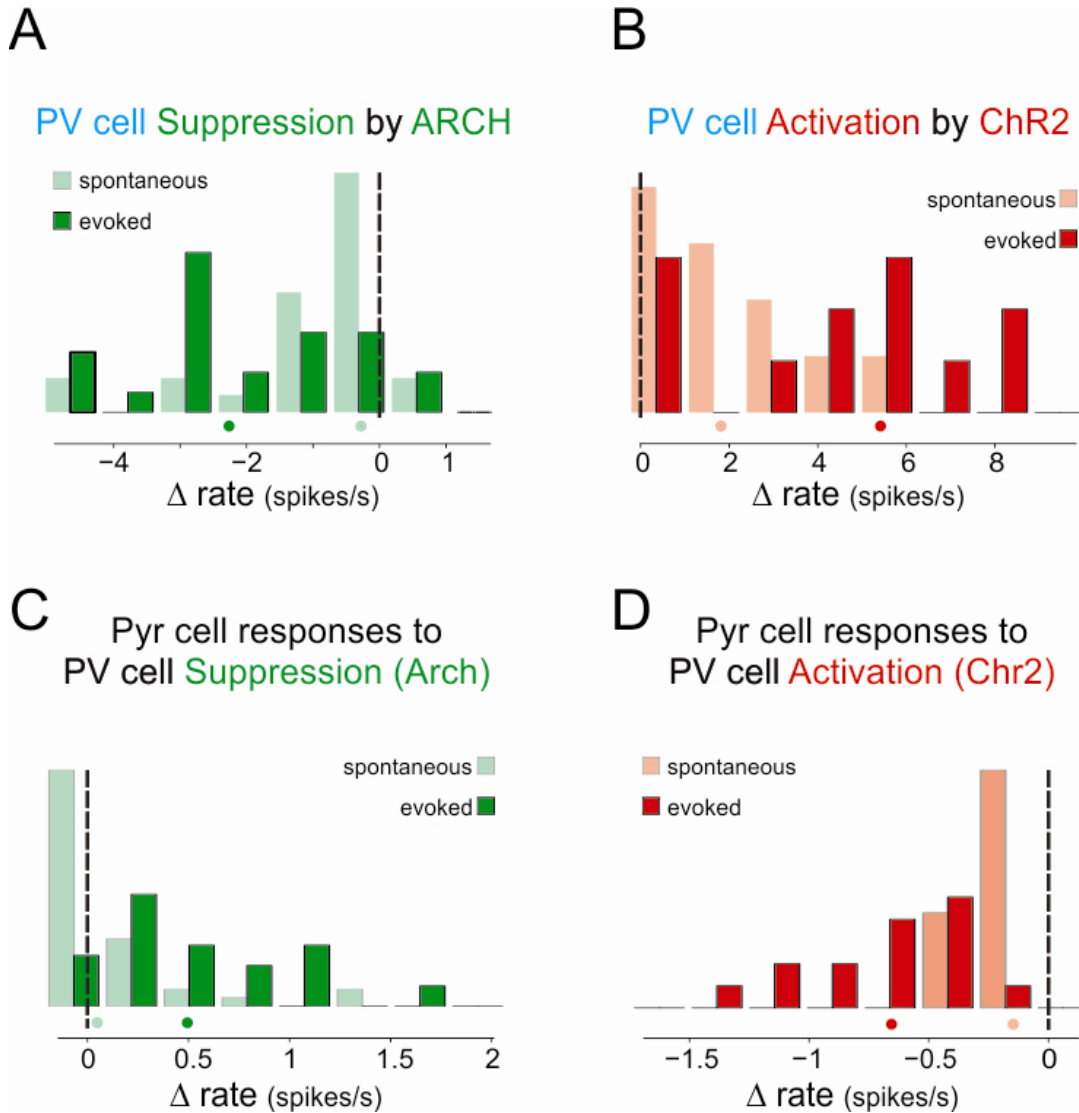
Figure S2: Quantification of visually evoked PV and Pyr cell responses during bi-directional control of PV cells (related to Figure 2)

(A) Histogram of change in the spontaneous and visually evoked firing rates of PV cells during photo-stimulation of Arch (n = 31). Dots illustrate the median

(B) Histogram of change in the spontaneous and visually evoked firing rates of PV cells during photo-stimulation of ChR2 (n = 16). Dots illustrate the median

(C) Histogram of change in the spontaneous and visually evoked firing rates of Pyr cells during photo-suppression of PV cells (n = 43). Dots illustrate the median

(D) Histogram of change in the spontaneous and visually evoked firing rates of Pyr cells during photo-activation of PV cells (n = 19). Dots illustrate the median
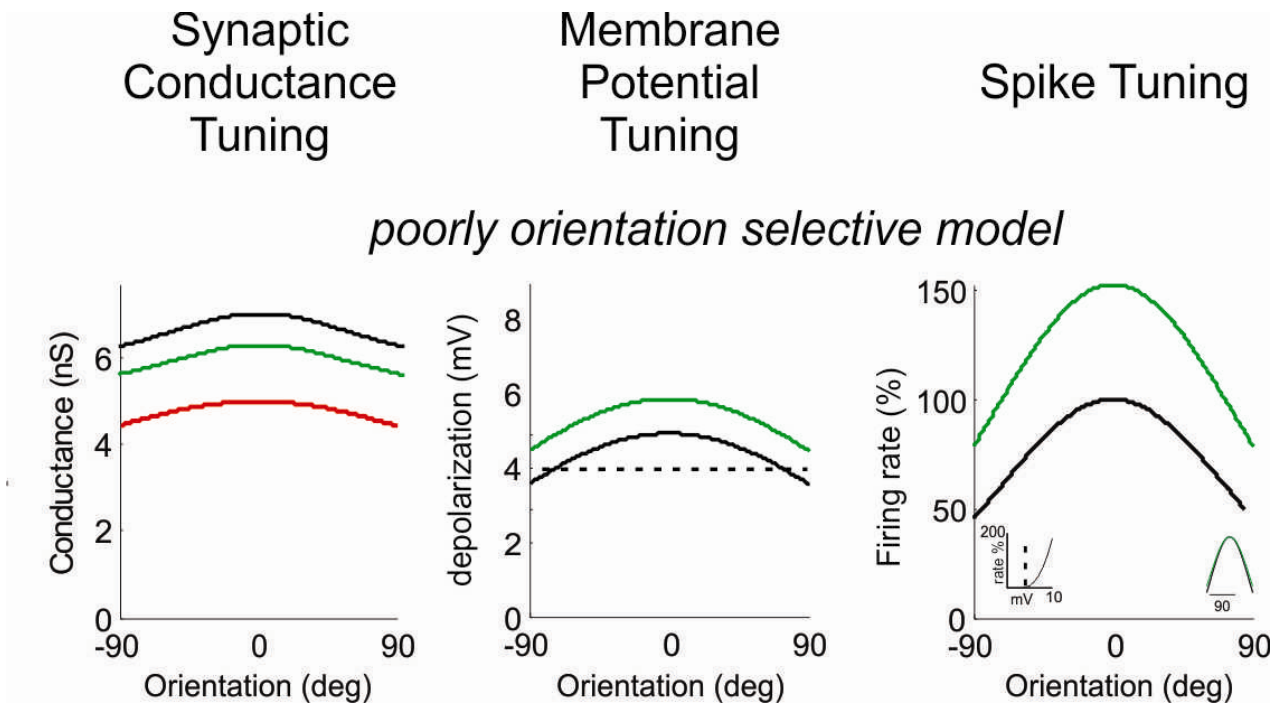
Figure S3: Simple conductance based model robustly captures linear transformation even for broadly orientation tuned Pyr cells (related to Figure 5)

Left, Modulation or tuning of excitatory (red) and inhibitory (black = control; green = upon PV cell suppression, i.e. 10% reduction in conductance) synaptic conductances as a function of orientation. The model cell's preferred orientation is defined to be at zero degrees.

Middle, Net depolarization in the membrane potential of modeled cell (resulting from conductances in on left) as a function of orientation under control conditions (black) and upon PV cell suppression (green). The dotted line illustrates the spiking threshold. Note under control conditions the majority of orientation tuned membrane potentials are already above threshold. Thus there is negligible change in tuning sharpness.

Right, Model cell's orientation tuning i.e. firing rate as a function of orientation under control conditions (black; OSI = 0.15; HWHH = 52 deg) and upon PV cell suppression (green; OSI = 0.12; HWHH = 49 deg). Left inset: illustrates the expansive nonlinear threshold or power law, i.e. the firing rate as a function of net membrane potential depolarization. Right inset, orientation tuning curves normalized to the peak. Note the decrease in inhibition by 10%, as experimentally determined, results in ~ 50% increase in spiking response at the preferred orientation, a modest decrease in orientation selectivity (ΔOSI = 0.03) and a negligible change in tuning sharpness: (ΔHWHH = 3 deg).
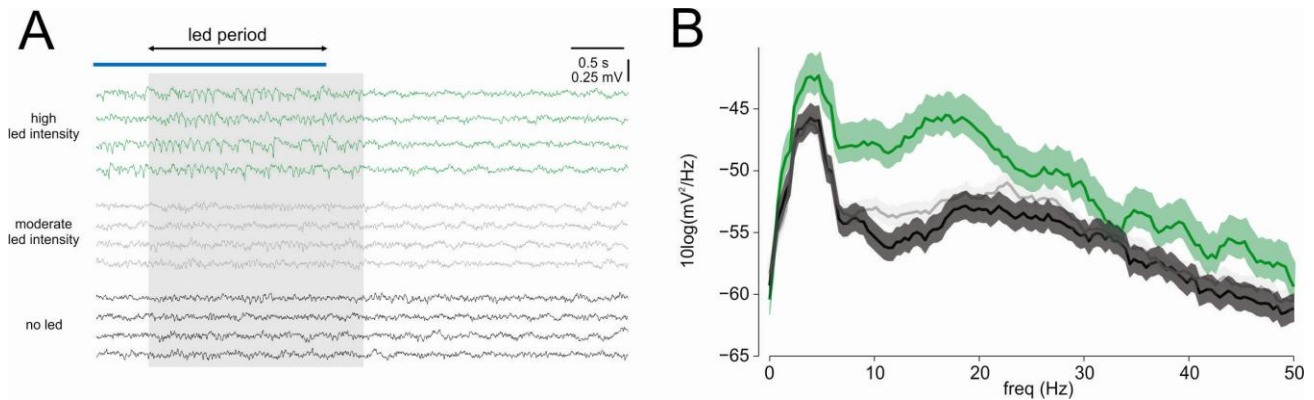
Figure S4: Local field potential during photo-stimulation of Arch in PV cells (related to Figure 2)

(A) Individual visually evoked local field potential (LFP) recorded in 150 μm from pia in during interleaved trials: control (black), moderate led intensity (gray, light intensity 0.1-0.5 mW/mm^2), and strong led intensity (green, light intensity > 5 mW/mm^2). Gray area: Stimulus presentation; Horizontal bars: Blue: LED illumination; Black: overlap between stimulus presentation and LED illumination.

(B) Fourier analysis of LFP during the overlap between stimulus presentation and LED illumination (shaded area are 95% confidence interval). Note that while there are slight changes in visually evoked LFP during moderate PV cell suppression, strong PV cell suppression results in a peak in LFP power between 15-20 Hz. We avoided this potentially aberrant response by only subtly suppressing PV cell activity (by a few spikes/s on average; Fig. 2) using moderately light intensity.

A spontaneous activity / visually evoked activity

B visually evoked / orientation selectivity / tuning sharpness / contrast exponent / spontaneous

Pyr control response
(PV cells expressing Arch)

Pyr control response
(PV cells experssing ChR2)
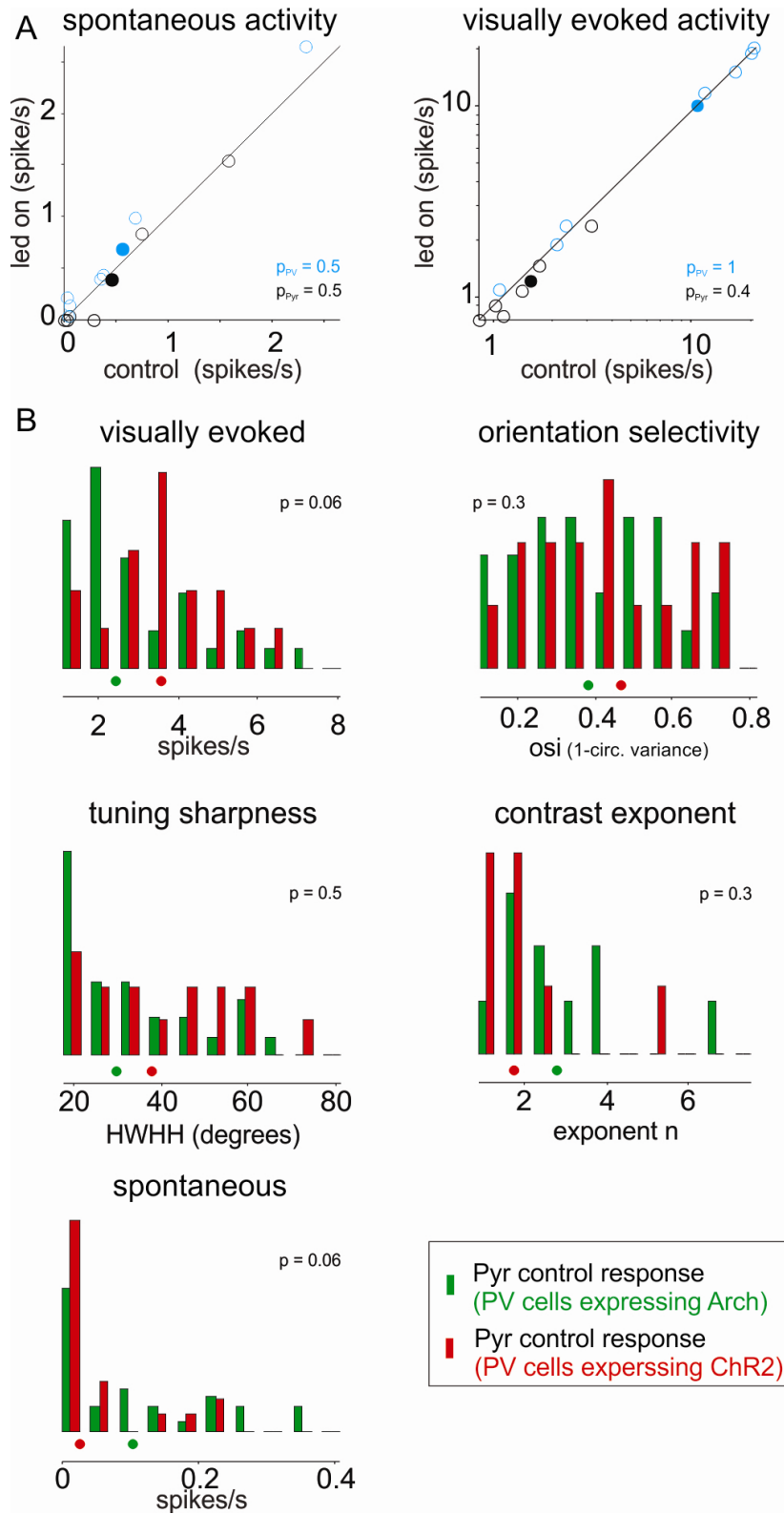
Figure S5: Controls: Cortical illumination has no effect on non-virally injected control mice; Expression of opsins does not impact layer 2/3 Pyr cell responses in the absence of cortical illumination (related to Figure 3).

(A) Targeted loose-patch recordings from PV and Pyr cells in PV-Cre x tdTomato mice that did not express either Chr2 or Arch. Scatter-plot PV (blue) and Pyr (black) cell illustrate spontaneous (left) and visually evoked (right, note log-scale) activity from control versus during 470nm led illumination of the cortex. Open symbols: individual cells; Closed symbols: average
Additionally, we found that cortical illumination did not impact any other tuning properties of Pyr and PV cells as indicated by the following p-values: orientation selectivity index: Pyr: p = 0.6; PV: p = 0.1, direction selectivity index: Pyr: = 0.8; PV: p = 1). Note that to ensure that the light intensity in these experiments was set at 5 mW/mm^2, approximately 10 times higher than the light levels used when perturbing PV cell activity.

(B) Histograms illustrate the distribution of various Pyr response properties under control conditions (i.e. *no* cortical illumination) in mice expressing either Arch (green; n = 31) or Chr2 (red; n = 14) in PV cells. Note the lack of significant difference between the two groups.